MOLECULAR AND CELLULAR BIOLOGY, June 2010, p. 3086–3098 Vol. 30, No. 12
0270-7306/10/$12.00 doi:10.1128/MCB.01652-09

Semaphorin 3E Initiates Antiangiogenic Signaling through Plexin D1 by Regulating Arf6 and R-Ras▽†

Atsuko Sakurai,[1] Julie Gavard,[2,3] Yuliya Annas-Linhares,[1] John R. Basile,[1] Panomwat Amornphimoltham,[4] Todd R. Palmby,[1] Hiroshi Yagi,[1] Fan Zhang,[5] Paul A. Randazzo,[6] Xuri Li,[5] Roberto Weigert,[4] and J. Silvio Gutkind[1]*

Oral and Pharyngeal Cancer Branch, National Institute of Dental and Craniofacial Research, National Institutes of Health, 30 Convent Drive, Room 211, Bethesda, Maryland 20892[1]; Institut Cochin, Universite Paris Descartes, CNRS (UMR 8104), Paris, France[2]; INSERM, U567, Paris, France[3]; Intracellular Membrane Trafficking Unit, Oral and Pharyngeal Cancer Branch, National Institute of Dental and Craniofacial Research, National Institutes of Health, 30 Convent Drive, Room 303A, Bethesda, Maryland 20892[4]; Unit on Retinal Vascular Neurobiology, National Eye Institute, National Institutes of Health, 5635 Fisher Lane, Rockville, Maryland 20852[5]; and Laboratory of Cellular and Molecular Biology, Center for Cancer Research, National Cancer Institute, Building 37, Room 2042, Bethesda, Maryland 20892[6]

Received 23 December 2009/Returned for modification 1 February 2010/Accepted 2 April 2010

Recent studies revealed that a class III semaphorin, semaphorin 3E (Sema3E), acts through a single-pass transmembrane receptor, plexin D1, to provide a repulsive cue for plexin D1-expressing endothelial cells, thus providing a highly conserved and developmentally regulated signaling system guiding the growth of blood vessels. We show here that Sema3E acts as a potent inhibitor of adult and tumor-induced angiogenesis. Activation of plexin D1 by Sema3E causes the rapid disassembly of integrin-mediated adhesive structures, thereby inhibiting endothelial cell adhesion to the extracellular matrix (ECM) and causing the retraction of filopodia in endothelial tip cells. Sema3E acts on plexin D1 to initiate a two-pronged mechanism involving R-Ras inactivation and Arf6 stimulation, which affect the status of activation of integrins and their intracellular trafficking, respectively. Ultimately, our present study provides a molecular framework for antiangiogenesis signaling, thus impinging on a myriad of pathological conditions that are characterized by aberrant increase in neovessel formation, including cancer.

Pathological angiogenesis characterizes numerous human diseases, ranging from chronic inflammation, atherosclerosis, diabetic retinopathy, and age-related macular degeneration to cancer (5, 11, 30). Thus, elucidating the mechanisms underlying normal and aberrant blood vessel growth may provide new therapeutic options for many highly prevalent disease conditions. Ultimately, normal angiogenesis results from a precise balance between pro- and antiangiogenic mediators. Among the former, the family of vascular endothelial growth factors (VEGFs), basic fibroblastic growth factor (bFGF), sphingosine-1-phosphate (S1P), and the chemokines interleukin-8/CXCL8 and SDF-1/CXCL12 and their receptors are some of the most widely investigated (reviewed in references 3, 5, 8, and 17). The best-known angiogenesis inhibitors are proteolytic cleavage products of extracellular matrix (ECM) or serum components, such as endostatin, angiostatin, arresten, and tumstatin (reviewed in references 11 and 20). Antiangiogenic cytokines have also been described, including interferons and certain interleukins, which appear to act indirectly by limiting the expression of proangiogenic mediators or inducing antiangiogenic molecules (reviewed in references 11 and 20). In contrast, there are few known developmentally regulated, naturally occurring antiangiogenic molecules, which include platelet factor 4 (18), thrombospondin 1 (14), and pigment epithelium-derived factor (PEDF) (9). Their precise mechanism of action is not fully understood, thus limiting the ability to design new molecularly based antiangiogenic strategies.

Emerging evidence suggests that proteins involved in transmitting axonal guidance cues, including members of the netrin, slit, eph, and semaphorin families, also play a critical role in blood vessel guidance during physiological and pathological blood vessel development (6). For example, multiple secreted class III semaphorins, which regulate developmental axonal growth (23, 27), are now known to act through their receptors, the A family plexins (plexins A1, A2, and A3), and their coreceptors, neuropilin 1 and neuropilin 2, to initiate pro- and antiangiogenic responses (reviewed in references 6 and 19). However, neuropilins also act as coreceptors for multiple angiogenic factors, such as VEGF, thus limiting our ability to distinguish the downstream signaling events initiated by semaphorins from those resulting from their interplay with endothelial growth and motility factors (19). In this regard, recent studies revealed that a class III semaphorin, semaphorin 3E (Sema3E), acts through a single-pass transmembrane receptor, plexin D1, independently of neuropilins to control endothelial cell (EC) positioning and patterning of the developing vasculature (13, 15). These findings prompted us to explore whether Sema3E acts as a natural antiangiogenic molecule and, if so, to

* Corresponding author. Mailing address: Oral and Pharyngeal Cancer Branch, National Institute of Dental and Craniofacial Research, National Institutes of Health, 30 Convent Drive, Rm. 211, MSC 4340, Bethesda, MD 20892. Phone: (301) 496-6259. Fax: (301) 402-0823. E-mail: sg39v@nih.gov.

† Supplemental material for this article may be found at http://mcb.asm.org/.

▽ Published ahead of print on 12 April 2010.

investigate the underlying molecular mechanism. Indeed, we show here that Sema3E is a potent inhibitor of adult and tumor-induced angiogenesis. Sema3E causes filopodial retraction in endothelial tip cells and inhibits endothelial cell adhesion by disrupting integrin-mediated adhesive structures. At the molecular level, this process involves the stimulation of plexin D1 by Sema3E, which in turn interferes with R-Ras function and leads to the rapid activation of Arf6, thus revealing a novel physiological antiangiogenic signaling route.

MATERIALS AND METHODS

Cell culture. Primary human umbilical vascular endothelial cells (HUVECs) were grown in endothelial cell medium, EGM-2 BulletKit (Cambrex Co.). Simian virus 40 (SV-40) immortalized murine vascular endothelial cells (SVECs), simian fibroblasts (COS-7), immortalized HUVECs (Eahy926), and HEK-293T cells were grown in Dulbecco's modified Eagle's medium (DMEM) (Sigma) plus 10% fetal bovine serum (FBS) (Sigma).

Expression vectors, siRNA, and transfection. Human plexin D1 cDNA (KIAA0620) was provided by T. Nagase. Full-length plexin D1 was subcloned into the pCEFL vector as an Asp718-NotI fragment, generating pCEFL-plexin D1-expressing plasmid. Plexin D1 GAPm, in which three key arginine residues involved in Ras GAP activity were mutated into alanine at amino acids 1484, 1485, and 1770, corresponding to the intracellular portion of human plexin D1, was generated using the QuikChange II XL site-directed mutagenesis kit (Stratagene). pCEFL-EGFP and a membrane-targeted enhanced green fluorescent protein (EGFP) expression vector (pCEFL-EGFP-CAAX) were generated by inserting a CAAX sequence from K-Ras into EGFP and subcloned into the pCEFL vector. pCMV-Sport6-Sema3E, the expression vector for mouse Sema3E, was obtained from Invitrogen (MGC full-length clone identifier [ID] 5357516). The 6×His and Myc tag sequences were amplified by PCR from the pSecTag2 vector (Invitrogen) and inserted between the internal EcoRI site of Sema3E and NotI at the C terminus of Sema3E. pXS-Arf6-HA-Q67L, pXS-Arf6-HA-T27N, and pRFP-CAAX were provided by J. G. Donaldson. pCXN2-FLAG-R-Ras and pERed-FLAG-R-RasGAP were provided by N. Mochizuki. TurboFect reagent (Fermentas) and Lipofectamine reagent (Invitrogen) were used for transfection of HEK-293T and COS-7 cells, respectively. The following predesigned small interfering RNAs (siRNAs) were used: AllStars negative-control siRNA, human R-Ras, mouse Arf6, and human Arf6 (Qiagen) and mouse plexin D1 (Invitrogen). The cells were transfected with control or with two independent siRNAs targeting different sequences of the molecule using Lipofectamine RNAiMAX transfection reagent (Invitrogen). After incubation for 4 to 5 days, the cells were used for the experiments. All results are representative of two independent siRNA sequences per target gene.

Reagents and antibodies. Recombinant mouse VEGF ($VEGF_{164}$), bFGF, and Sema3E/Fc chimeric protein were from R&D systems. Alexa Fluor-labeled phalloidin and isolectin B4 were from Invitrogen. Glass coverslips or cell culture surfaces were coated with 10 μg/ml of poly-L-lysine (Sigma), type I rat tail collagen (BD Biosciences), or human plasma fibronectin (Invitrogen). The following antibodies were used. Rabbit anti-plexin D1 was generated by using synthetic peptides corresponding to amino acids 1652 to 1672 of human plexin D1. This anti-plexin D1 antiserum does not cross-react with other endothelial plexins, plexins B1, B2, and B3 (data not shown). Rabbit anti-Arf6 was provided by J. G. Donaldson. Rabbit anti-R-Ras was provided by N. Mochizuki. Other antibodies were mouse antitubulin; rabbit anti-focal adhesion kinase (anti-FAK) (Santa Cruz); mouse antihemagglutinin (anti-HA) (Covance); mouse anti-FLAG (Sigma); goat anti-plexin D1 (Abcam); rat anti-mouse CD29, clone 9EG7, mouse anti-CD29, clone 18/CD29, and mouse antipaxillin (BD Transduction Laboratories); anti-human β1-integrin, clone LM534 (Millipore); and mouse anti-phospho-Y397 FAK (Biosource).

Production of Sema3E conditioned medium. HEK-293T cells were transfected with pCMV-Sport6-Sema3E-HisMyc and cultured in serum-free DMEM. After 24 h, conditioned medium was collected, filtered, and used for the COS-7 collapse assay. Conditioned medium collected from pCEFL-EGFP-transfected HEK-293T cells was used as a control.

Intraocular injection and cornea pocket assay. Intraocular injection was performed as described previously (12) using postnatal day 5 (P5) pups, except that the pups were sacrificed 6 h after injection. The endothelial cells extending filopodia at the developing front of the retinal vasculature were counted as tip cells. The mouse cornea assay was performed as described previously (4), using 10-week-old female C57BL/6 mice. Micropellets containing 35 ng of VEGF and 35 ng of bFGF with or without 180 ng of Sema3E were implanted into mouse corneal micropockets. The blood vessel growth was photographed and analyzed on day 4 after implantation.

DIVAA. Directed *in vivo* angiogenesis assays (DIVAA) were performed as described previously (2). Briefly, angioreactors were filled with 200 μl of Cultrex-reconstituted basement membrane substrate (Trevigen) containing 12.5 ng of VEGF and 37.5 ng bFGF or HN12 cells (2×10^5 cells) with or without 100 ng/ml of recombinant Sema3E. The angioreactors were implanted subcutaneously into 6-week-old nude mice (Jackson Laboratory). Fourteen days after implantation, the mice were sacrificed, the angioreactors were removed and photographed, and the length of blood vessel ingrowth into angioreactors was measured.

Endothelial cell sprouting assay. In order to generate endothelial cell spheroids of defined size and cell numbers, SVECs were suspended in DMEM containing 10% FBS and 0.25% (wt/vol) carboxymethylcellulose and seeded in nonadherent round-bottom 96-well plates (Becton Dickinson Labware). Under these conditions, all suspended cells formed a single EC spheroid within 24 h. The standardized spheroids were collected and used for the *in vitro* sprouting assay. Briefly, SVEC spheroids (750 cells/spheroid) were harvested, embedded in type I collagen gel, and cultured for 48 h after the addition of VEGF (30 ng/ml)- and bFGF (30 ng/ml)-containing DMEM with or without Sema3E (100 ng/ml). The cumulative length of all capillary-like sprouts originating from the central plain of an individual spheroid was measured at ×10 magnification using a digitized imaging system (Axiovision; Carl Zeiss, Inc.).

Live-cell imaging. SVEC or COS-7 cells transfected with plasmids as indicated in the figure legends were plated onto fibronectin-coated coverslips, serum starved, and stimulated with Sema3E (100 ng/ml). The cells were imaged on an Olympus IX-81 inverted confocal microscope. To monitor the cell shape, a fluorescence image was obtained every 20 s, and a series of time lapse images were converted into video format using MetaMorph software (Molecular Devices).

Immunofluorescence microscopy. The cells cultured on fibronectin-coated coverslips were serum starved and treated with Sema3E (100 ng/ml) for 30 to 120 min, fixed with 3.7% formaldehyde in phosphate-buffered saline (PBS) for 30 min, and permeabilized with 0.05% Triton X-100 for 10 min. The cells were blocked with 3% FBS-containing PBS for 30 min and incubated with the indicated antibodies for 1 h at room temperature. Immunopositive reactions were visualized with Alexa Fluor 488-labeled secondary antibody (Invitrogen). Actin was visualized using Alexa Fluor 546-conjugated phalloidin (Invitrogen). Samples were mounted in Vectashield DAPI (4′,6-diamidino-2-phenylindole)-containing mounting medium (Vector Laboratories) and visualized under an Axio Imager Z1 microscope equipped with an ApoTome system controlled by AxioVision software (Carl Zeiss). Colocalization of plexin D1 and R-Ras was imaged and quantified under an LSM 700 confocal microscope with Zen software (Carl Zeiss).

Cell adhesion assay. Endothelial cell adhesion was assessed by measuring endogenous alkaline phosphatase activity by using the Atto-Phos AP fluorescent substrate system (Promega) as described previously (24). COS-7 cells were transfected with control or plexin D1-expressing plasmids, together with firefly luciferase. After 24 h, the cells were detached by brief exposure to trypsin and suspended in control or Sema3E-containing conditioned medium and then plated on plates coated with ECM as indicated in the figures. After 15 min, nonadherent cells were removed by washing the plates with PBS four times; adhered cells were lysed, and luciferase activity was measured. The adherent cells were quantified by measuring luciferase activity and are shown as a fold increase over control conditioned-medium-treated samples.

Integrin internalization assay. The internal accumulation of β1-integrin was monitored as described previously (22), using HUVECs and monitoring the internalization of anti-human β1-integrin (clone LM534). Briefly, HUVECs were grown on fibronectin-coated coverslips and serum starved overnight. The mouse anti-human β1-integrin was diluted in 0.01% bovine serum albumin (BSA) (United States Biological)-containing DMEM to a final concentration of 5 μg/ml and then added to the cells at 4°C for 30 min to label surface integrin. Excess antibody was removed by washing the cells two times with ice-cold 0.01% BSA-DMEM, and the cells were stimulated with 100 ng/ml Sema3E at 37°C for the time indicated. The cells were fixed immediately (surface integrin) or washed with acid wash buffer (pH 2.2, 100 mM glycine, 20 mM magnesium acetate, 50 mM KCl) for 60 s to remove noninternalized surface integrin and then washed with PBS twice and fixed (internalized integrin). The cells were incubated with Alexa Fluor 488-conjugated anti-mouse IgG in 0.2% saponin-containing PBS, and fluorescence images were collected using an Axio Imager Z1 microscope equipped with an ApoTome system. The number of cells exhibiting at least six or more acid-resistant β1-integrin-positive vesicle-like structures was determined ($n > 100$).

COS-7 collapse assay. COS-7 cells were grown on a 6-well tissue culture plate and cotransfected with 0.5 μg of pCEFL-EGFP and 2 μg of pCEFL-plexin D1. The cells were serum starved for 6 h and treated with Sema3E-containing conditioned medium for 30 min. The cells were fixed with 3.7% formaldehyde and visualized under a fluorescence microscope. Cell collapse was scored for about 150 EGFP-positive cells for each experimental condition in triplicate wells, and the percentage of collapsed cells was calculated.

GST pulldown assays. R-Ras and Arf6 activation was monitored by glutathione *S*-transferase (GST) pulldowns by using GST-RalGDS (Ras binding domain of RalGDS) and GST-GGA3 (Arf binding domain of GGA3) recombinant proteins, respectively, bound to glutathione slurry resin (Amersham Bioscience). Cells were lysed in buffer containing 50 mM Tris-HCl, pH 7.5, 100 mM NaCl, 2 mM $MgCl_2$, 0.1% SDS, 0.5% sodium deoxycholate, 1% Triton X-100, 10% glycerol, and protease inhibitor cocktail (Sigma). Precleared lysates were incubated with slurry resin. The resin was washed three times in lysis buffer, and the proteins collected on the resin were subjected to SDS-PAGE, followed by immunoblotting with the indicated antibodies.

Immunoprecipitation assay. COS-7 cells were transfected with expression vectors for plexin D1 and R-Ras. After 24 h, the cells were pretreated with 10 μM $AlCl_3$ and 10 mM sodium fluoride for 5 min and then stimulated with Sema3E-containing conditioned medium for 30 min. The cells were washed with PBS and lysed with ice-cold lysis buffer (20 mM Tris-HCl, pH 7.5, 150 mM NaCl, 20 mM $MgCl_2$, 1 mM sodium vanadate, 1% Triton X-100, 10 μM $AlCl_3$, 10 mM sodium fluoride) including 1/100 dilution of protease inhibitor cocktail (Sigma). Precleared cell lysates were incubated with anti-plexin D1 antibody. Immunoprecipitates collected on protein G-Sepharose were subjected to SDS-PAGE and immunoblotting with antibodies as indicated.

RESULTS

Sema3E inhibits angiogenesis *in vivo*. We first sought to examine whether Sema3E can affect the growth of blood vessels, taking advantage of the fact that in the eye the development of the retinal vasculature occurs postnatally in mice. This process involves the sprouting of new vessels, with endothelial tip cells that extend numerous filopodia and respond to attractive and repulsive guidance cues at the leading edge of the new branching blood vessels, while the neighboring stalk cells proliferate and form the vascular lumen (12). Intraocular injections of recombinant Sema3E into P5 mice led to disorganized retinal vasculature with increased vessel diameter (Fig. 1A). Remarkably, Sema3E treatment decreased both the number of filopodia per tip cell and the number of filopodium-extending tip cells at the angiogenic front. Sema3E alone did not induce angiogenesis in a mouse cornea pocket assay, while exogenously supplied VEGF and bFGF induced the formation of readily visible blood vessels (Fig. 1B, arrowheads). Notably, the coadministration of Sema3E inhibited the formation of neovessels in the otherwise avascular cornea (Fig. 1B). We further tested the antiangiogenic potential of Sema3E using a tumor-angiogenesis assay (DIVAA) that enables the quantitative assessment of functional vessel growth in small silicone tubes or angioreactors filled with ECM components implanted in mice. Significant blood vessel growth occurred in angioreactors containing VEGF and bFGF (Fig. 1C, left), similar to that caused by HN12 angiogenic head and neck cancer cells (Fig. 1C, right), as previously reported (2). Both growth factor-induced angiogenesis and cancer cell-induced angiogenesis were significantly reduced by Sema3E (Fig. 1C), together supporting the idea that Sema3E displays potent antiangiogenic properties.

Sema3E induces endothelial cell retraction. Western blot analysis revealed that plexin D1 is expressed in primary human endothelial cells (HUVEC), as well as immortalized human and murine endothelial cell lines (Fig. 2A), using HEK-293T cells transfected with plexin D1 as a positive control. Treatment of endothelial spheroids cultured in three-dimensional (3D) collagen gels with VEGF- and bFGF-induced capillary sprouting, which was significantly inhibited by Sema3E (Fig. 2B and C), suggesting that Sema3E displays direct antiangiogenic properties on endothelial cells *in vitro*. Knockdown of plexin D1 by siRNA rescued Sema3E-induced capillary sprouting inhibition (Fig. 2D and E), consistent with the role of plexin D1 as a Sema3E receptor (15). Sema3E also dramatically affected the endothelial cell morphology, as judged by using endothelial cells transfected with membrane-targeted red fluorescent protein (RFP) (RFP-CAAX) and monitoring their shape by time-lapse microscopy. Exposure of endothelial cells to Sema3E caused rapid membrane retraction, and subsequently, cells detached from the ECM and collapsed (Fig. 2F; see Movie S1 in the supplemental material). The cells remained viable, and this process was reversible upon washing the cells with fresh culture medium (not shown). Sema3E had limited impact on confluent endothelial cells in monolayers (not shown) but caused a remarkable change in the shape and actin cytoskeleton of subconfluent endothelial cells, including the rapid dissolution of actin-based stress fibers (Fig. 2G and H). These results suggest that Sema3E induces the rapid endothelial cell retraction, likely by regulating the actin cytoskeleton.

Sema3E negatively regulates cell-ECM adhesive interaction. As Sema3A, another member of the class III semaphorins, inhibits endothelial cell motility by controlling integrin function (25), we then analyzed focal adhesions (FAs), which are dynamic cell-to-ECM adhesive structures containing integrins. After 15 min of Sema3E treatment, most FAs, which were visualized by paxillin staining, were rapidly dispersed, concomitant with decreased actin stress fibers (Fig. 3A). Sema3E treatment markedly decreased the phosphorylation of FAK, a key molecule controlling FA turnover (16), at tyrosine 397 (Y397), which is a major autophosphorylation site in FAK (Fig. 3B). Sema3E-induced FAK inactivation was further confirmed by Western blotting for pY397-FAK, and this response to Sema3E was prevented in plexin D1 knockdown cells (Fig. 3C). Furthermore, plexin D1 knockdown rescued both Sema3E-induced FA and actin stress fiber disassembly (Fig. 3D).

Next, we examined the effect of Sema3E on β1-integrin, which mediates cell-ECM interactions in endothelial cells and is required for angiogenesis (1). Staining for active β1-integrin using an antibody that recognizes its ligand-competent conformation was clearly decreased in Sema3E-treated cells (Fig. 3E, top). However, the total amount of β1-integrin was unchanged (Fig. 3E, bottom). This observation prompted us to investigate the localization of β1-integrin in Sema3E-treated cells. For these experiments, we incubated HUVECs with nonfunctional monoclonal antibody against human β1-integrin to label cell surface integrin. When stimulated with Sema3E, β1-integrin accumulated in an internal vesicular pool (Fig. 3G). Knockdown of plexin D1 by siRNA blocked Sema3E-induced β1-integrin internalization in these human endothelial cells (Fig. 3F and H). Based on these results, we hypothesized that Sema3E might induce the rapid β1-integrin inactivation and internalization, thereby negatively regulating endothelial cell adhesion to the ECM. Indeed, exposure to Sema3E inhibited attachment of endothelial cells to type I collagen, a ligand for

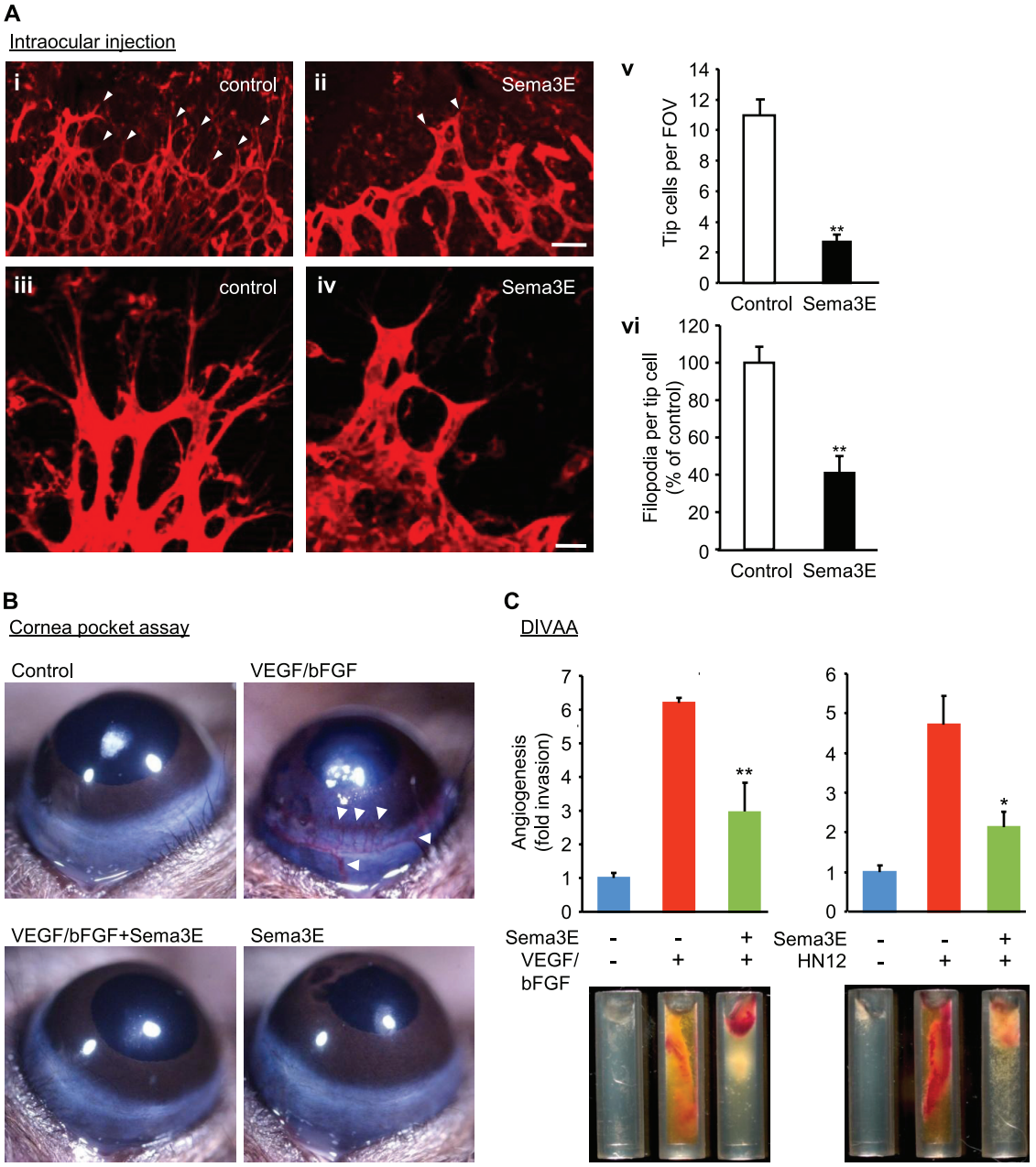

FIG. 1. Sema3E inhibits angiogenesis *in vivo*. (A) Isolectin B4-stained retinal vasculature in control (i and iii) or 1 μg Sema3E-injected (ii and iv) P5 retinas. The number of filopodium-extending tip cells (arrowheads) was decreased in Sema3E-injected eyes. (iii and iv) Higher magnifications of tip cells show the retraction of filopodia in Sema3E-injected eyes. (v) The number of tip cells per field of view (FOV). The data shown are means plus standard errors of the mean (SEM); **, $P < 0.01$; $n = 7$. (vi) The number of filopodia per tip cell. The data shown are means plus SEM; **, $P < 0.01$; $n = 11$. (B) Cornea pocket assay. VEGF- and bFGF-induced blood vessel growth was inhibited by Sema3E. The images were taken on day 4 following implantation of pellets in the eyes of 10-week-old mice. (C) VEGF and bFGF (left) or highly angiogenic head and neck cancer cells (HN12 cells) (right) were mixed with basement membrane extract, either alone or in combination with Sema3E, and implanted into nude mice following the DIVAA protocol. Representative images of each experimental group are shown. Blood vessel invasion into the angioreactors is shown as fold increase over PBS control samples. The data shown are means plus SEM. $n = 5$; *, $P < 0.05$; **, $P < 0.01$. Scale bars, 50 μm (i and ii) and 20 μm (iii and iv).

β1-integrin, while the cell adhesion to poly-L-lysine, which is integrin independent, was not affected (Fig. 3I).

Sema3E induces cytoskeletal collapse in an integrin-dependent fashion. The cytoskeletal collapse of COS-7 cells transfected with neuropilins and plexins can recapitulate semaphorin-mediated repulsive signaling (26). Using this reconstitution system, we explored the signal transduction pathways by which Sema3E-plexin D1 causes cell retraction. When COS-7 cells were cotransfected with control or plexin D1-expressing plasmids and membrane-targeted EGFP (EGFP-CAAX), only the cells expressing plexin D1 exhibited a collapse phenotype upon Sema3E stimulation, as reflected by their decreased cell surface (Fig. 4A).

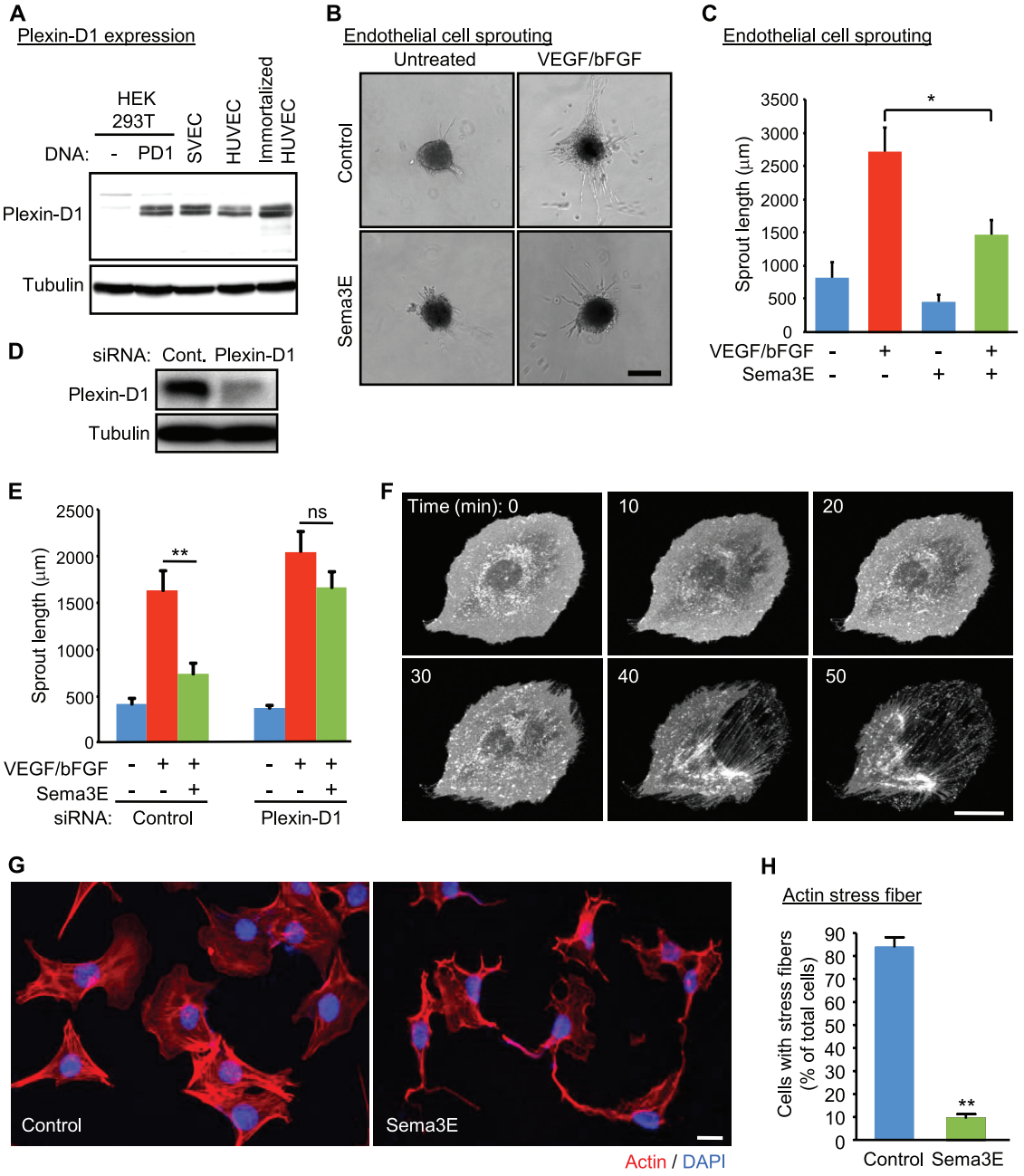

FIG. 2. Sema3E induces endothelial cell retraction. (A) Immunoblot analysis for plexin D1 in diverse endothelial cells. The lysates of plexin D1-transfected HEK-293T cells were used as a positive control. Tubulin was used as a loading control. (B) Spheroid-based three-dimensional *in vitro* angiogenesis assay. Endothelial cell spheroids were embedded in collagen gels and cultured in the presence of VEGF and bFGF, with or without Sema3E. A representative image of each experimental group is shown. Scale bar, 200 μm. (C) The cumulative length of all capillary-like sprouts originating from the central plain of an individual spheroid was measured. The data shown are means plus SEM; $n = 10$; *, $P < 0.05$. (D) siRNA-mediated knockdown of plexin D1 in SVECs. Plexin D1 protein levels were assessed 4 days later. Cont., control. (E) Control or plexin D1 siRNA-transfected cells were subjected to a sprouting assay as described for panels B and C. The data shown are means plus SEM; $n = 10$; **, $P < 0.01$; ns, no significant difference. (F) Sequential time-lapse images of the retraction of SVECs expressing RFP-CAAX upon Sema3E stimulation. Scale bar, 20 μm. (G) SVECs were treated with Sema3E for 2 h and stained for F-actin. Scale bar, 20 μm. Most cells showed a reduction in stress fibers after Sema3E treatment. (H) Quantification of panel E. The cells exhibiting actin stress fibers were counted. The data represent the percentages plus SEM. **, $P < 0.01$.

COS-7 cells do not express neuropilin 1 and neuropilin 2 endogenously, and expression of these neuropilins was not sufficient to support Sema3E-induced cell collapse, nor did their coexpression with plexin D1 affect this response to Sema3E (not shown). Together, this suggested that expression of plexin D1 in these cells is necessary and sufficient to initiate Sema3E signaling. Next, we monitored the cellular changes caused by Sema3E using time-lapse imaging. COS-7 cells were either transfected with control

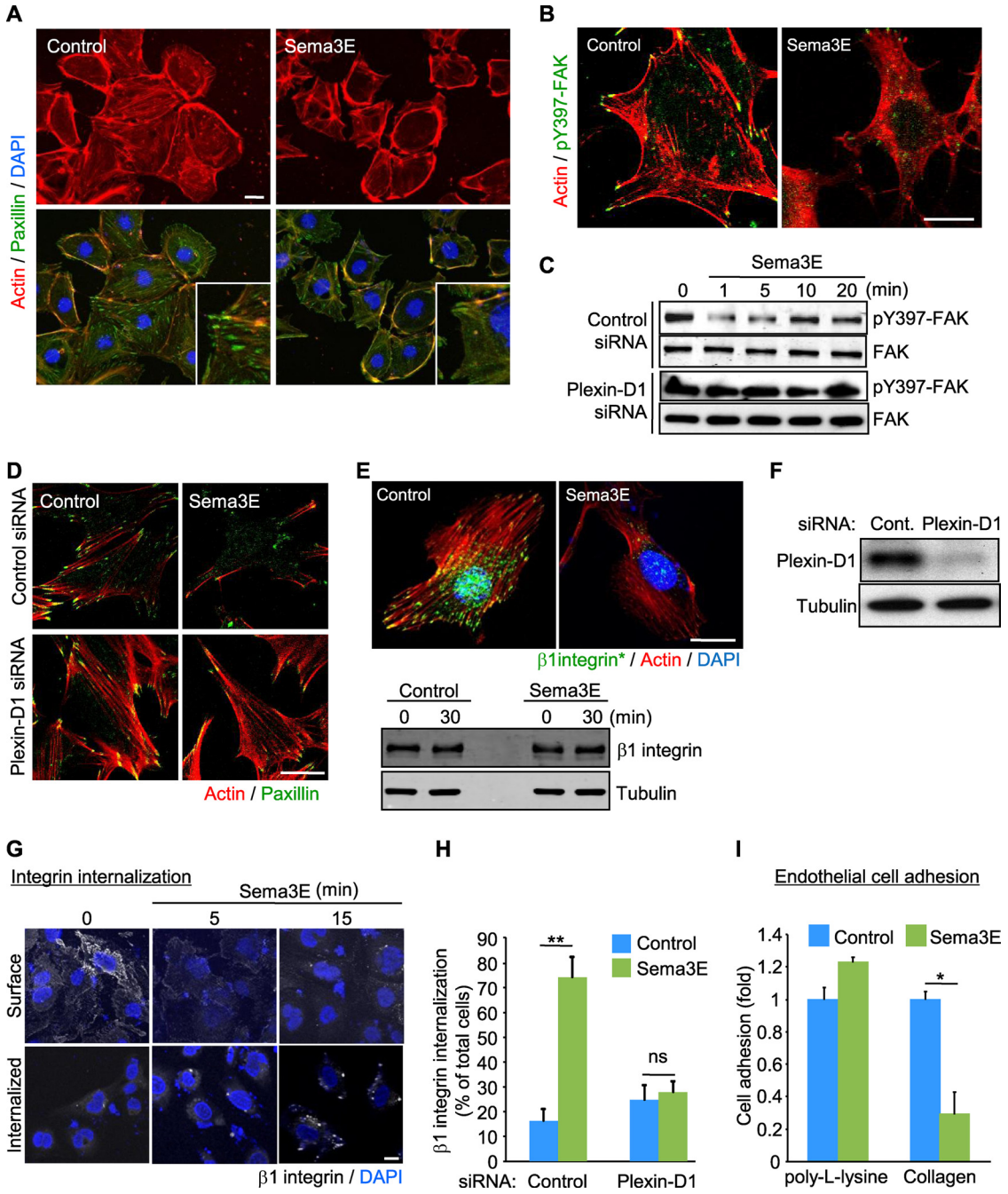

FIG. 3. Sema3E negatively regulates cell-ECM adhesive interactions. (A and B) SVECs were serum starved, treated with Sema3E for 15 min, and stained for F-actin (red) and paxillin (green) (A) or phospho-FAK (pY397-FAK) (green) (B). Insets show higher magnifications of the corresponding images. (C) Control or plexin D1 siRNA-transfected SVECs were serum starved and treated with Sema3E, and total cell lysates were tested for pY397-FAK and total FAK. (D) siRNA-transfected SVECs were serum starved, treated with Sema3E, and stained for F-actin (red) and paxillin (green). (E) Serum-starved SVECs were treated with Sema3E for 30 min and stained for active β1-integrin (green) and F-actin (red) (top panel). The total amount of β1-integrin protein was unchanged (bottom panel). (F) siRNA-mediated knockdown of plexin D1 in HUVECs. Plexin D1 protein levels were assessed 4 days later. (G) HUVECs were incubated with mouse anti-β1-integrin to label cell surface β1-integrin and then incubated with Sema3E for the indicated periods. The cells were fixed immediately (Surface) or subjected to acid wash (Internalized) before fixation to remove membrane-bound antibodies, and β1-integrin was visualized by Alexa Fluor 488-conjugated anti-mouse IgG antibody. (H) Control or plexin D1 siRNA-transfected HUVECs were subjected to an integrin internalization assay as described for panel G. The internalized β1-integrin was visualized and quantified as described in Materials and Methods. Scale bars, 20 μm. The graphs represent means plus SEM of three independent experiments. ns, no significant difference; **, $P < 0.01$. (I) Adhesion of SVECs to a poly-L-lysine- or type I collagen-coated dish in the presence or absence of Sema3E was measured as described in Materials and Methods. The data shown are means plus SEM. *, $P < 0.05$. Scale bars, 20 μm.

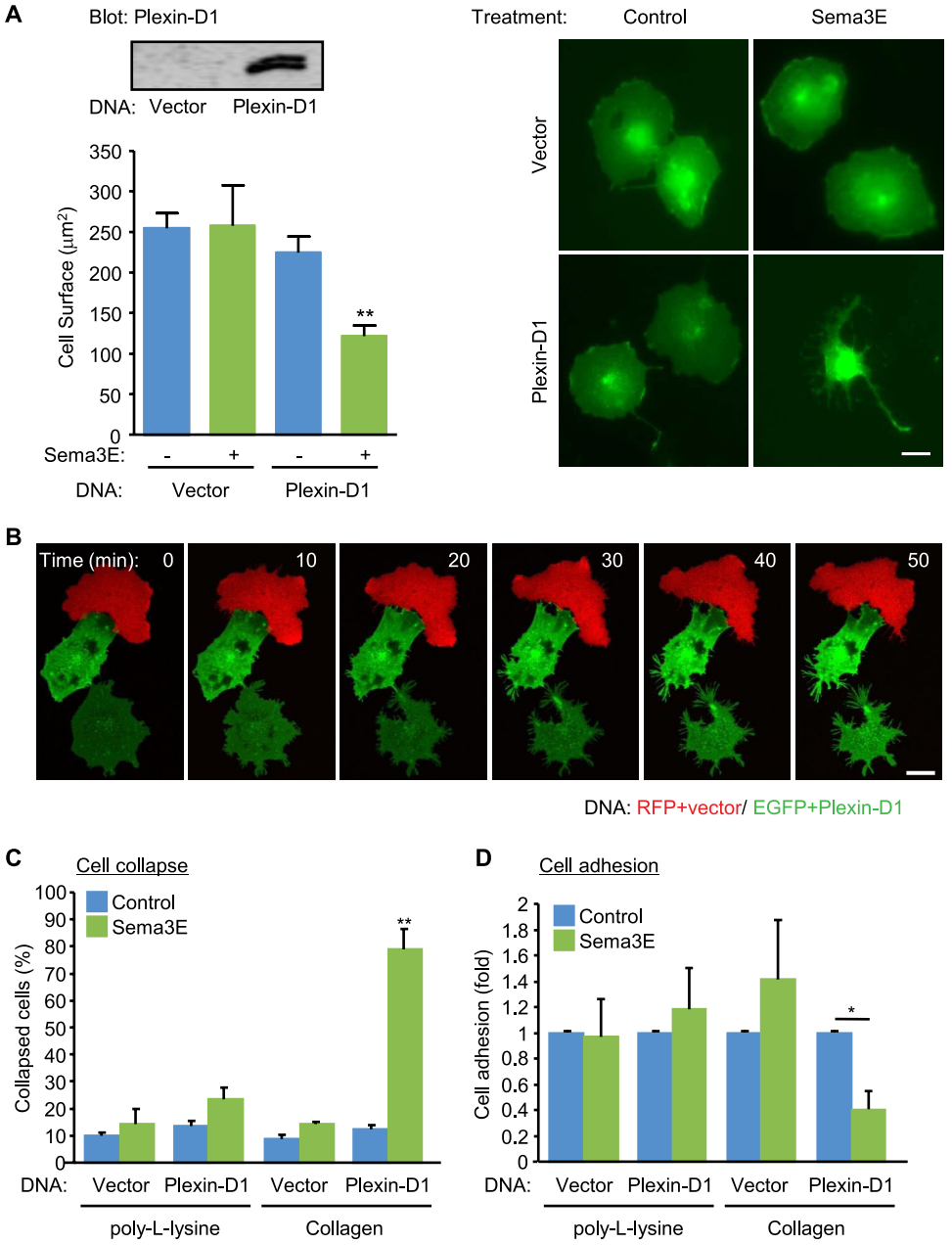

FIG. 4. Sema3E induces cell collapse via plexin D1 in an integrin-dependent fashion. (A) COS-7 cells were transfected with control or plexin D1-expressing plasmids, together with EGFP-CAAX, and the protein expression was analyzed by Western blotting with anti-plexin D1 antibody (upper left). The cells were serum starved and stimulated with Sema3E-containing conditioned medium for 30 min and fixed, and the cell surface area of EGFP-positive cells ($n > 150$) was measured. The graph shows the average cell surface area plus SEM from three independent experiments; **, $P < 0.01$. (B) Time-lapse images of Sema3E-stimulated COS-7 cells expressing the indicated plasmids. Only plexin D1-expressing cells collapsed upon simulation. (C) COS-7 cells were plated on poly-L-lysine- or type I collagen-coated dishes, and cell collapse was assessed as for panel A. EGFP-positive cells exhibiting a collapse phenotype were scored as a percentage of the total number of transfected cells. The data shown are means plus SEM of three independent experiments. **, $P < 0.01$. (D) COS-7 cells were transfected with control or plexin D1-expressing plasmids, and cell adhesion to poly-L-lysine- or type I collagen-coated dishes in the presence or absence of Sema3E was measured as described in Materials and Methods. The data represent means plus SEM. *, $P < 0.05$. Scale bars, 20 μm.

plasmid and RFP-CAAX (Fig. 4B, red cell) or with plexin D1 and EGFP-CAAX (Fig. 4B, green cells), plated on fibronectin-coated coverslips, and stimulated with Sema3E. Plexin D1-expressing cells started shrinking within 10 min of Sema3E stimulation, with a remarkable remodeling of the plasma membrane and multiple intracellular membrane compartments (Fig. 4B; see Movie S2 in the supplemental material). After 30 min, the cells had shrunk and were less spread than their adjacent control cell (red), which showed only some scatter membrane ruffling. Plexin D1-expressing cells started collapsing from the opposite side of cell-to-cell contacts, aligned with the observation that Sema3E affects primarily isolated endothelial cells or tip cells in developing vessels *in*

vivo. Sema3E-induced cell collapse was integrin dependent, as cells plated on poly-L-lysine did not collapse (Fig. 4C). Consistent with the result for endothelial cells, the adhesion of COS-7 cells ectopically expressing plexin D1 to collagen type I was inhibited by Sema3E, while cell adhesion to poly-L-lysine was not affected (Fig. 4D). These data further support the emerging possibility that Sema3E might negatively regulate cell adhesion to ECM by modulating integrin function.

The R-Ras GAP activity of plexin D1 is necessary but not sufficient for Sema3E-induced cell collapse. Most plexins harbor an intrinsic GTPase-activating protein (GAP) activity toward R-Ras (21, 28, 29). As R-Ras activation promotes cell adhesion by activating integrins, it can be hypothesized that R-Ras inactivation by plexins may reduce integrin-dependent cell adhesion, thus inducing cell collapse (reviewed in reference 19).The cytoplasmic domains of plexins have a split Ras GAP domain that includes three highly conserved arginine residues essential for their R-Ras GAP activity (21). Thus, we generated mutant constructs for plexin D1 (plexin D1 GAPm) containing R1484A, R1485A, and R1770A substitutions (Fig. 5A). COS-7 cells expressing plexin D1 GAPm showed slight changes in the morphology but did not collapse in response to Sema3E on collagen or fibronectin (Fig. 5B to D), both of which bind integrins. Similarly, Sema3E did not inhibit the adhesion of plexin D1 GAPm-expressing cells to fibronectin (Fig. 5E). These results suggested that inactivation of R-Ras may be required for Sema3E-induced changes in cell-ECM adhesion. However, we could not detect a decrease in R-Ras activity upon Sema3E stimulation (Fig. 5F, lane 2). Although unexpected, these findings are aligned with a very recent study in which plexin D1 inactivated R-Ras only when coexpressed with members of the Rnd family of Rho GTPases (29). However, the fact that cell collapse and inhibition of cell adhesion in COS-7 cells upon Sema3E stimulation do not require the coexpression of Rnd1 or Rnd2 prompted us to examine in more detail the role of the plexin D1 R-Ras GAP function in mediating the biological responses to Sema3E.

First, to confirm the biochemical assays, we exogenously introduced R-Ras GAP in COS-7 cells and examined the GTP–R-Ras level using pulldown approaches. A relatively low level of expression of an R-Ras GAP was sufficient to inactivate R-Ras strongly (Fig. 5F). However, these R-Ras GAP-expressing cells showed slight changes in their morphology but did not display a collapse phenotype, which was readily observed in plexin D1-expressing cells upon Sema3E stimulation (Fig. 5G and H). R-Ras GAP-expressing cells showed loose attachment to the ECM, but that was observed only when large amounts of R-Ras GAP were overexpressed for prolonged periods of time. Aligned with the observations in COS-7 cells, Sema3E did not change endogenous active R-Ras levels in endothelial cells (Fig. 5I). Notably, although plexin D1 does not reduce R-Ras–GTP levels, it coimmunoprecipitates with R-Ras in response to Sema3E when expressed in COS-7 cells, which was not observed in the plexin D1 GAPm (Fig. 5J). Furthermore, double staining showed that endogenous plexin D1 and R-Ras colocalized in an intracellular vesicular compartment in response to Sema3E in endothelial cells (Fig. 5K). Taken together, these observations suggested that the physical interaction between plexin D1 and R-Ras mediated by the RasGAP motif in plexin D1, likely sequestering R-Ras rather than accelerating the hydrolysis of GTP bound to R-Ras, may contribute to Sema3E-induced cell collapse. While this possibility is under investigation, these findings also suggested that inhibition of R-Ras function alone might not be sufficient to mediate the responses to Sema3E.

Plexin D1 activates Arf6, a novel plexin D1 effector contributing to Sema3E signaling in endothelial cells. We next explored the possibility that molecular events other than decreased R-Ras–GTP levels may contribute to plexin D1-initiated signaling. In this regard, we observed that Sema3E causes a subtle and delayed decrease in the basal levels of the GTP-bound forms RhoA and Rac1 GTPases, but multiple approaches leading to the inhibition of RhoA and Rac1 were also not sufficient to cause COS-7 cell collapse or to mimic the effects of Sema3E in endothelial cells (not shown). In search of a molecular mechanism underlying the biological responses elicited by Sema3E, we focused our attention on another small GTPase, Arf6, as this member of the Arf family GTPases regulates the trafficking of β1-integrin, and its inhibition compromises both cell adhesion and migration (10, 22). Indeed, the expression of a dominant-negative Arf6 mutant, Arf6 T27N, abolished Sema3E-induced cell collapse, while expression of the active Arf6 mutant, Arf6 Q67L, alone (not shown) or together with plexin D1, was sufficient to induce ligand-independent collapse of the transfected cells (Fig. 6A to C). Surprisingly, pulldown assays revealed that Sema3E activates endogenous Arf6 within 1 min in plexin D1-transfected COS-7 cells (Fig. 6D). This rapid Arf6 activation was not observed in plexin D1 GAPm-transfected COS-7 cells (Fig. 6D), suggesting R-Ras–plexin D1 binding is required for plexin D1-induced Arf6 activation. Similarly, Sema3E induced remarkable and rapid Arf6 activation in endothelial cells (Fig. 6E), which required plexin D1 expression, as it was prevented by plexin D1 knockdown (Fig. 6F and 2D). In addition, R-Ras silencing limited Sema3E-induced Arf6 activation, thus complementing the data obtained in COS-7 cells using plexin D1 GAPm mutants (see Fig. S1 in the supplemental material). Furthermore, Sema3E failed to provoke the dissolution of FA and the disassembly of stress fibers in cells expressing reduced levels of Arf6 (Fig. 6G to I). Arf6 silencing also significantly limited the ability of Sema3E to promote β1-integrin internalization (Fig. 6K to M) and to inhibit the attachment of endothelial cells to fibronectin and collagen I (Fig. 6J and data not shown). Taken together, these results suggest that the Sema3E-plexin D1-Arf6 signaling axis may initiate an antiangiogenic response by disrupting the formation of adhesive structures, thereby preventing the attachment of endothelial cells to their ECM and interfering with the growth of new sprouting vessels (Fig. 7).

DISCUSSION

The recent discovery that axon guidance molecules also play a key role in developmental and postnatal angiogenesis has provided an opportunity to identify novel molecular mechanisms that can be exploited to understand and treat various human diseases that are characterized by aberrant angiogenesis. In this regard, multiple class III semaphorins act through plexin A and its coreceptors, neuropilin 1 and neuropilin 2, to regulate endothelial cell function (reviewed in reference 19). The nature of the pro- and antiangiogenic signals initiated by

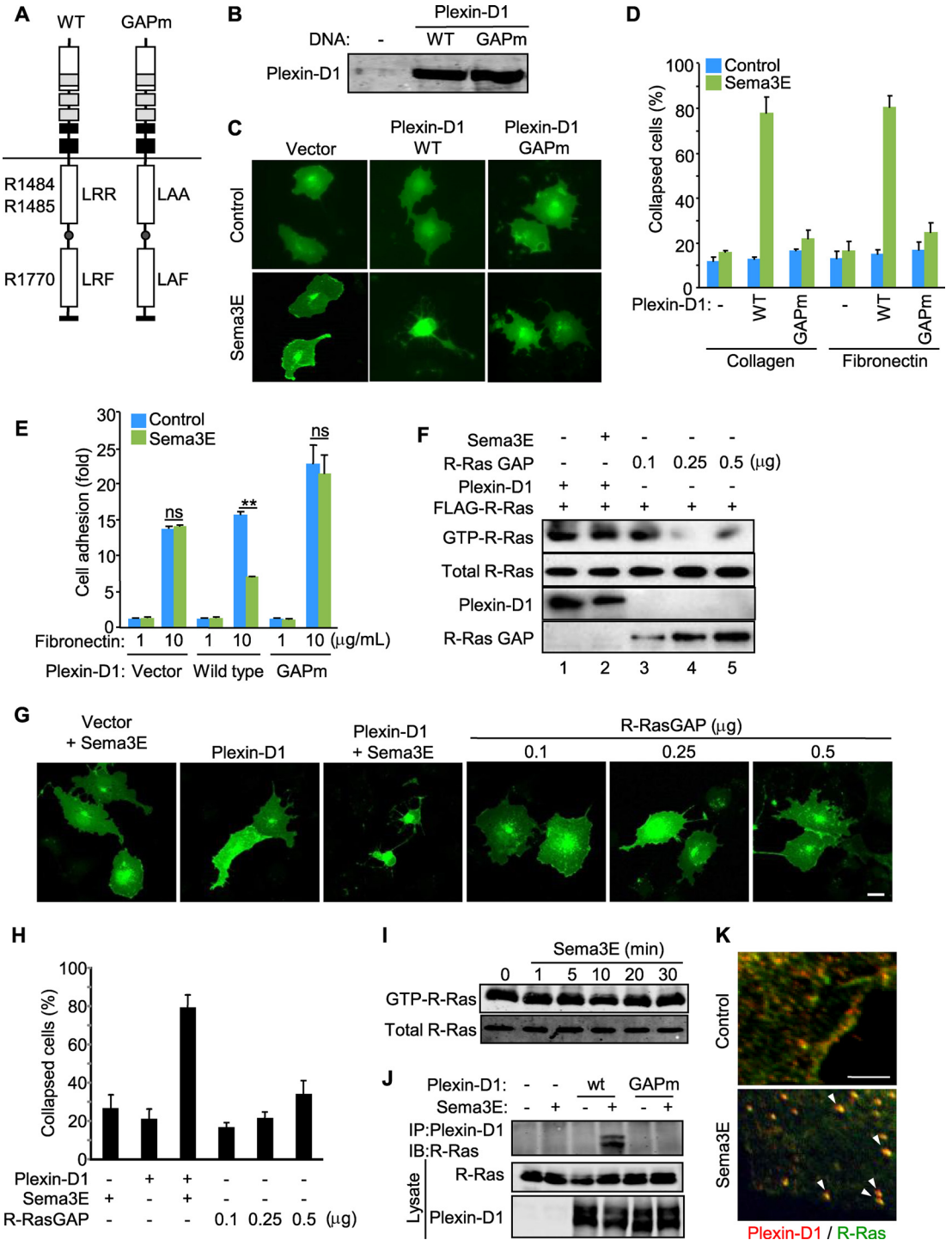

FIG. 5. R-Ras inactivation is not sufficient for cytoskeletal collapse. (A) Schematic representation of the plexin D1 constructs. WT, wild type; GAPm, R-Ras GAP mutant. The numbers indicate amino acid residue positions in the domains. A, Ala; F, Phe; L, Leu; R, Arg. (B) Protein expression of plexin D1 constructs in COS-7 cells. (C and D) COS-7 cells were plated on type I collagen- or fibronectin-coated dishes and transfected with EGFP-CAAX and the indicated plexin D1-expressing plasmids. A collapse assay was performed as described for Fig. 4C. (E) COS-7 cells were transfected with the indicated plasmids and subjected to an adhesion assay as described for Fig. 4D. ns, no significant difference; **, $P < 0.01$. (F) COS-7 cells were transfected with the indicated plasmids, serum starved, and stimulated with Sema3E for 15 min. R-Ras activity was measured by GST pulldown assay as described in Materials and Methods. The cells expressing even relatively low levels of R-Ras GAP resulted in effective inactivation of R-Ras. (G and H) COS-7 cells were transfected with GFP-CAAX and plasmids as for panel G and subjected to a collapse assay as described for Fig. 4C. (I) HUVECs were serum starved and stimulated with Sema3E, and R-Ras activity was measured by GST pulldown assay. (J) COS-7 cells were transfected with FLAG–R-Ras- and plexin D1-expressing plasmids, serum starved, exposed to aluminum fluoride, and stimulated with Sema3E for 30 min, followed by immunoprecipitation (IP) and immunoblotting (IB) using the indicated antibodies. (K) Serum-starved HUVECs were treated with Sema3E for 5 min and stained for plexin D1 (red) and R-Ras (green). In control cells, plexin D1 and R-Ras are localized at the plasma membrane and likely in cytoplasmic membrane compartments but rapidly colocalize in an intracellular vesicular compartment upon Sema3E stimulation. The arrowheads indicate sites of colocalization. Scale bars, 20 μm.

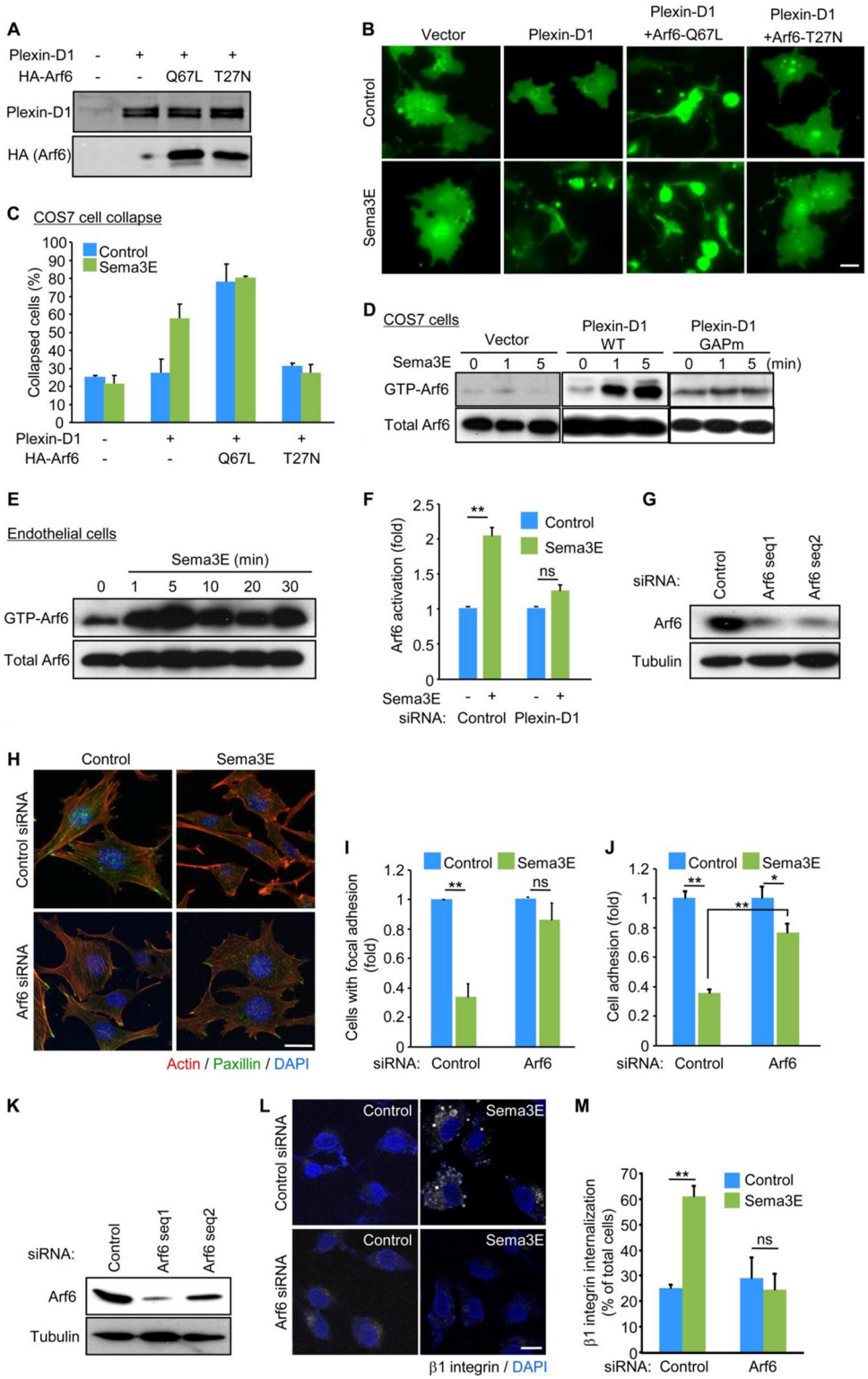

FIG. 6. Sema3E induces Arf6 activation in ECs. (A) Immunoblotting of plexin D1- and HA-tagged Arf6 in COS-7 cells. (B and C) COS-7 cells transfected with the indicated plasmids were subjected to a collapse assay as described for Fig. 4C. (D to F) COS7 cells transfected with control or plexin D1 vectors (D), SVECs (E), and plexin D1 siRNA-transfected SVECs (F) were serum starved and stimulated with Sema3E, and Arf6 activity was measured as described in Materials and Methods. GTP-Arf6 levels were normalized to the amount of total Arf6. (G to J) siRNA-mediated knockdown of Arf6 in SVECs. Arf6 protein levels were assessed 4 days later. (H) siRNA-transfected SVECs were serum starved, stimulated with Sema3E, and stained for F-actin (red) and paxillin (green). (I) The number of cells with FAs was scored as a percentage of the total cell number. (J) Adhesion of siRNA-transfected SVECs to fibronectin was measured as described for Fig. 3I. (K to M) siRNA-mediated knockdown of Arf6 in HUVECs. Arf6 protein levels were assessed 5 days later. (L) siRNA-transfected cells were subjected to an integrin internalization assay as described for Fig. 3G. (M) The internalized β1-integrin was visualized and quantified as described in Materials and Methods. Scale bars, 20 μm. The graphs represent means plus SEM of three independent experiments. ns, no significant difference; **, $P < 0.01$.

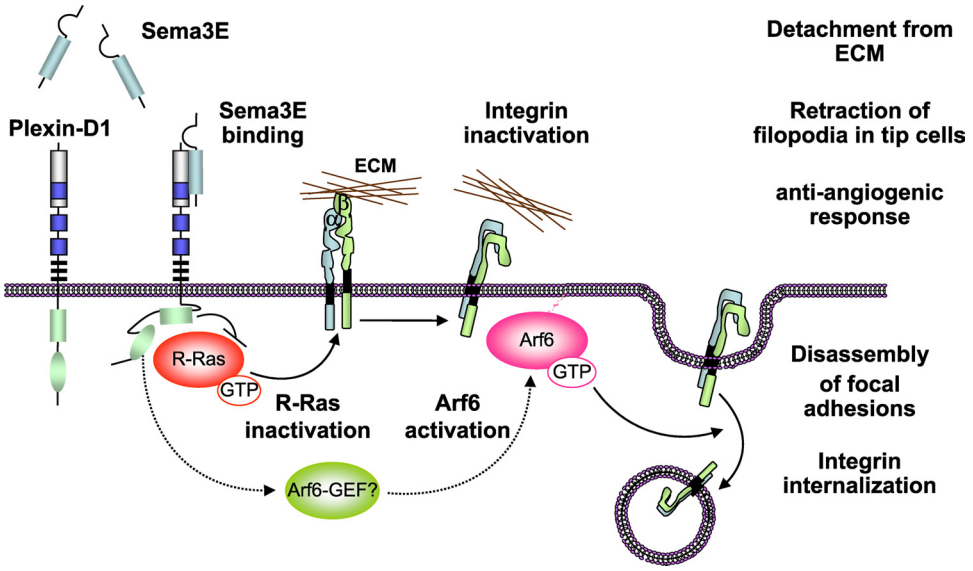

FIG. 7. Schematic representation of the antiangiogenic Sema3E-plexin D1 signaling pathway in endothelial cells. The activation of plexin D1 by Sema3E induces the association of the Ras GAP domain of plexin D1 with R-Ras, thus sequestering R-Ras, and promotes the rapid activation of Arf6, likely by stimulating Arf6 GEFs. This results in the inactivation of integrins and their subsequent internalization, respectively, thus inhibiting endothelial cell adhesion to the ECM by disrupting integrin-mediated adhesive structures and causing filopodial retraction in endothelial tip cells. Ultimately, this two-pronged mechanism by which the Sema3E-plexin D1 signaling system acts may provide a repulsive cue for endothelial cells, thereby providing protection from the aberrant sprouting and growth of new blood vessels.

these semaphorin receptors is still poorly understood, as neuropilins also associate with multiple VEGF receptors, including VEGFR1, VEGFR2, and VEGFR3; hence, these semaphorins may act, at least partially, by interfering with VEGF binding to its receptors and coreceptors and its signaling capacity (19). Here, we took advantage of the fact that Sema3E acts directly on a single-pass transmembrane receptor, plexin D1, and that developmental studies in model organisms indicate that deficiencies in plexin D1 and Sema3E causes aberrant vascular patterning to dissect how Sema3E regulates endothelial cell biology. We show here that Sema3E acts on plexin D1 in endothelial cells to induce detachment and retraction of the cells from ECM, thereby displaying potent antiangiogenic properties *in vivo*. At the molecular level, we provide evidence that Sema3E causes the association of plexin D1 with R-Ras and the concomitant activation of Arf6 and that this interferes with the ability of integrin to bind the ECM, thus causing FA disassembly and endothelial cell detachment. This, in turn, may contribute to the ability of Sema3E to block the sprouting of endothelial cells, the formation of filopodia, migration of tip cells, and the inability of tumor cells to promote neovascularization, thus blocking tumor-induced angiogenesis.

The cytoplasmic domains of plexins share a Ras GAP homology region and a GTPase binding domain that associates with Rho GTPases, such as Rnd1 and Rac1 (19). Plexins function as R-Ras GAPs and downregulate R-Ras activity, thereby inhibiting integrin-mediated cell adhesion and inducing repulsive responses in neuronal cells (21). In the B-family plexins, this R-Ras GAP domain acts in coordination with the activation of RhoA through a C-terminal PDZ binding motif by which plexin B associates with RhoGEFs, as we and others have recently documented (reviewed in reference 19). Plexin A, instead, associates with neuropilin 1 and FARP2 (FERM, RhoGEF, and pleckstrin domain protein 2), a GEF for Rac1, and the consequent Rac1 activation results in the enhanced binding of Rnd1 to plexin A1 and the stimulation of its R-Ras GAP activity (28).

However, plexin D1 exerts its R-Ras GAP activity only when coexpressed with Rnd2 (29). Nonetheless, plexin D1 does not require the expression of Rnd subfamily GTPases to cause cell collapse (this study and reference 15). While the R-Ras GAP activity of plexin D1 may not be strictly required for its function, mutations in the arginine finger prevented the initiation of the biological responses elicited by Sema3E. Indeed, we provide evidence that plexin D1 may utilize its Ras GAP domain to sequester R-Ras, even if it does not decrease cellular GTP–R-Ras levels in the absence of Rnd proteins. This proposed mechanism of action may result in a targeted and localized inhibition of R-Ras function, rather than in a global inhibition of R-Ras. Of note, inhibition of R-Ras by overexpressing a specific R-Ras GAP was not sufficient to cause cell collapse or cell detachment from the ECM. Instead, we found that plexin D1 causes the rapid and potent activation of Arf6 and that Arf6 function is strictly necessary for plexin D1-initiated cell collapse in COS-7 cells and for FA disassembly, attachment inhibition, and integrin internalization in response to Sema3E in endothelial cells.

The precise mechanism by which plexin D1 activates Arf6 is at present unknown. R-Ras inhibition by overexpression of its GAP is not sufficient to stimulate Arf6 (not shown), suggesting that Arf6 activation is not an immediate downstream event caused by R-Ras inhibition. On the other hand, R-Ras silencing in endothelial cells limited Sema3E-induced Arf6 stimulation, and plexin D1 GAPm does not activate Arf6, suggesting that the plexin D1–R-Ras interaction is required to trigger

Arf6 activation. Of interest, R-Ras knockdown in endothelial cells diminished, but did not abolish, Arf6 activation by Sema3E, suggesting that in these cells there might be compensation by other members of the R-Ras subfamily, such as TC21/R-Ras2 or M-Ras/R-Ras3. Indeed, we observed that HUVECs express a high level of TC21 (data not shown). Overall, it is possible that the Sema3E-dependent association of plexin D1 with R-Ras may trigger a conformation change in plexin D1 that results in the activation of additional signaling events leading to Arf6 stimulation. Numerous Arf6 GEFs and GAPs control the activity of Arf6, which could mediate the activation of this GTPase upon binding of plexin D1 to R-Ras. Among them, three families of Arf6 GEFs, brefeldin-resistant Arf GEF (BRAG), Arf nucleotide binding site opener (ARNO)/cytohesin, and exchange factor for Arf6 (EFA6), can activate Arf6 (7). Each of these GEFs is expressed in multiple isoforms and splice variants, which are likely functionally redundant, thus preventing their analysis by knockdown strategies. Instead, we have begun analyzing the contribution of these GEFs to Arf6 activation by using dominant-negative mutants, including ARNO, EFA6, and BRAG2/GEP100. Among them, the dominant-negative mutant of BRAG2/GEP100 eliminates the activation of Arf6 and cell collapse in response to Sema3E (not shown), suggesting that members of the BRAG2/GEP100 family of Arf6 GEFs represent likely candidates to mediate these responses, albeit by a yet-to-be-identified mechanism. In this regard, while BRAG2/GEP100 can bind to tyrosine-phosphorylated epidermal growth factor receptor (EGFR), we did not detect any phosphorylation in tyrosine in plexin D1 upon Sema3E stimulation or BRAG2/GEP100 association with plexin D1. Thus, we can speculate that plexin D1 may regulate BRAG2/GEP100 by additional molecular intermediates, such as by the recruitment of adapter molecules or changes in lipid signaling mediators, an area that warrants further investigation.

The ability to establish integrin-dependent interactions with the ECM enables tip cells to migrate and lead the sprouting vessels by invading stromal tissue, resulting in the growth of new blood vessels (1, 12). In this regard, our findings suggest that Sema3E may act as a potent antiangiogenic factor by inducing filopodial retraction in endothelial tip cells, thus likely providing a repulsive cue preventing tumor-induced angiogenesis and suppressing excess vascularization during development and in adults. Our results also indicate that Sema3E acts on plexin D1 to initiate a two-pronged mechanism involving R-Ras inactivation and Arf6 stimulation, thereby affecting the activation status of integrins and their intracellular trafficking, respectively. Ultimately, our present study may provide a novel molecular framework for antiangiogenesis signaling, thus impinging on a myriad of pathological conditions that are characterized by aberrant increase in neovessel formation, including cancer.

ACKNOWLEDGMENTS

We thank C. J. Edgell (UNC), J. G. Donaldson (NIH, NHLBI, Bethesda, MD), N. Mochizuki (National Cardiovascular Center Research Institute, Osaka, Japan), and T. Nagase (Kazusa DNA Research Institute, Kisarazu, Japan) for providing reagents and D. Martin (NIH, NIDCR) and N. Mochizuki and S. Fukuhara (NCVC, Osaka, Japan) for comments and discussions.

A.S. was supported by JSPS postdoctoral fellowships for research abroad and Y.A.-L. by the Howard Hughes Scholars Program. This research was supported by the Intramural Research Program of the NIH, National Institute of Dental and Craniofacial Research, and National Eye Institute.

REFERENCES

1. **Avraamides, C. J., B. Garmy-Susini, and J. A. Varner.** 2008. Integrins in angiogenesis and lymphangiogenesis. Nat. Rev. Cancer. **8:**604–617.
2. **Basile, J. R., K. Holmbeck, T. H. Bugge, and J. S. Gutkind.** 2007. MT1-MMP controls tumor-induced angiogenesis through the release of semaphorin 4D. J. Biol. Chem. **282:**6899–6905.
3. **Belperio, J. A., M. P. Keane, D. A. Arenberg, C. L. Addison, J. E. Ehlert, M. D. Burdick, and R. M. Strieter.** 2000. CXC chemokines in angiogenesis. J. Leukoc. Biol. **68:**1–8.
4. **Cao, R., E. Brakenhielm, R. Pawliuk, D. Wariaro, M. J. Post, E. Wahlberg, P. Leboulch, and Y. Cao.** 2003. Angiogenic synergism, vascular stability and improvement of hind-limb ischemia by a combination of PDGF-BB and FGF-2. Nat. Med. **9:**604–613.
5. **Carmeliet, P.** 2005. Angiogenesis in life, disease and medicine. Nature **438:** 932–936.
6. **Carmeliet, P., and M. Tessier-Lavigne.** 2005. Common mechanisms of nerve and blood vessel wiring. Nature **436:**193–200.
7. **Casanova, J. E.** 2007. Regulation of Arf activation: the Sec7 family of guanine nucleotide exchange factors. Traffic **8:**1476–1485.
8. **Coultas, L., K. Chawengsaksophak, and J. Rossant.** 2005. Endothelial cells and VEGF in vascular development. Nature **438:**937–945.
9. **Dawson, D. W., O. V. Volpert, P. Gillis, S. E. Crawford, H. Xu, W. Benedict, and N. P. Bouck.** 1999. Pigment epithelium-derived factor: a potent inhibitor of angiogenesis. Science **285:**245–248.
10. **Dunphy, J. L., R. Moravec, K. Ly, T. K. Lasell, P. Melancon, and J. E. Casanova.** 2006. The Arf6 GEF GEP100/BRAG2 regulates cell adhesion by controlling endocytosis of beta1 integrins. Curr. Biol. **16:**315–320.
11. **Folkman, J.** 2007. Angiogenesis: an organizing principle for drug discovery? Nat. Rev. Drug Discov. **6:**273–286.
12. **Gerhardt, H., M. Golding, M. Fruttiger, C. Ruhrberg, A. Lundkvist, A. Abramsson, M. Jeltsch, C. Mitchell, K. Alitalo, D. Shima, and C. Betsholtz.** 2003. VEGF guides angiogenic sprouting utilizing endothelial tip cell filopodia. J. Cell Biol. **161:**1163–1177.
13. **Gitler, A. D., M. M. Lu, and J. A. Epstein.** 2004. PlexinD1 and semaphorin signaling are required in endothelial cells for cardiovascular development. Dev. Cell **7:**107–116.
14. **Good, D. J., P. J. Polverini, F. Rastinejad, M. M. Le Beau, R. S. Lemons, W. A. Frazier, and N. P. Bouck.** 1990. A tumor suppressor-dependent inhibitor of angiogenesis is immunologically and functionally indistinguishable from a fragment of thrombospondin. Proc. Natl. Acad. Sci. U. S. A. **87:**6624–6628.
15. **Gu, C., Y. Yoshida, J. Livet, D. V. Reimert, F. Mann, J. Merte, C. E. Henderson, T. M. Jessell, A. L. Kolodkin, and D. D. Ginty.** 2005. Semaphorin 3E and plexin-D1 control vascular pattern independently of neuropilins. Science **307:**265–268.
16. **Hamadi, A., M. Bouali, M. Dontenwill, H. Stoeckel, K. Takeda, and P. Ronde.** 2005. Regulation of focal adhesion dynamics and disassembly by phosphorylation of FAK at tyrosine 397. J. Cell Sci. **118:**4415–4425.
17. **Hla, T.** 2003. Signaling and biological actions of sphingosine 1-phosphate. Pharmacol. Res. **47:**401–407.
18. **Maione, T. E., G. S. Gray, J. Petro, A. J. Hunt, A. L. Donner, S. I. Bauer, H. F. Carson, and R. J. Sharpe.** 1990. Inhibition of angiogenesis by recombinant human platelet factor-4 and related peptides. Science **247:**77–79.
19. **Neufeld, G., and O. Kessler.** 2008. The semaphorins: versatile regulators of tumour progression and tumour angiogenesis. Nat. Rev. Cancer. **8:**632–645.
20. **Nyberg, P., L. Xie, and R. Kalluri.** 2005. Endogenous inhibitors of angiogenesis. Cancer Res. **65:**3967–3979.
21. **Oinuma, I., Y. Ishikawa, H. Katoh, and M. Negishi.** 2004. The Semaphorin 4D receptor Plexin-B1 is a GTPase activating protein for R-Ras. Science **305:**862–865.
22. **Powelka, A. M., J. Sun, J. Li, M. Gao, L. M. Shaw, A. Sonnenberg, and V. W. Hsu.** 2004. Stimulation-dependent recycling of integrin beta1 regulated by ARF6 and Rab11. Traffic **5:**20–36.
23. **Raper, J. A.** 2000. Semaphorins and their receptors in vertebrates and invertebrates. Curr. Opin. Neurobiol. **10:**88–94.
24. **Sakurai, A., S. Fukuhara, A. Yamagishi, K. Sako, Y. Kamioka, M. Masuda, Y. Nakaoka, and N. Mochizuki.** 2006. MAGI-1 is required for Rap1 activation upon cell-cell contact and for enhancement of vascular endothelial cadherin-mediated cell adhesion. Mol. Biol. Cell **17:**966–976.
25. **Serini, G., D. Valdembri, S. Zanivan, G. Morterra, C. Burkhardt, F. Caccavari, L. Zammataro, L. Primo, L. Tamagnone, M. Logan, M. Tessier-Lavigne, M. Taniguchi, A. W. Puschel, and F. Bussolino.** 2003. Class 3

semaphorins control vascular morphogenesis by inhibiting integrin function. Nature **424:**391–397.
26. **Takahashi, T., A. Fournier, F. Nakamura, L. H. Wang, Y. Murakami, R. G. Kalb, H. Fujisawa, and S. M. Strittmatter.** 1999. Plexin-neuropilin-1 complexes form functional semaphorin-3A receptors. Cell **99:**59–69.
27. **Tessier-Lavigne, M., and C. S. Goodman.** 1996. The molecular biology of axon guidance. Science **274:**1123–1133.
28. **Toyofuku, T., J. Yoshida, T. Sugimoto, H. Zhang, A. Kumanogoh, M. Hori, and H. Kikutani.** 2005. FARP2 triggers signals for Sema3A-mediated axonal repulsion. Nat. Neurosci. **8:**1712–1719.
29. **Uesugi, K., I. Oinuma, H. Katoh, and M. Negishi.** 2009. Different requirement for Rnd GTPases of R-Ras GAP activity of plexin-C1 and plexin-D1. J. Biol. Chem. **284:**6743–6751.
30. **Yancopoulos, G. D., M. Klagsbrun, and J. Folkman.** 1998. Vasculogenesis, angiogenesis, and growth factors: ephrins enter the fray at the border. Cell **93:**661–664.